PAPER NAME

Irzaman et al.2024Design and fabricatio n of photovoltaics based on MFS (AgBaT iO3silicon p-type) stru

WORD COUNT

5382 Words

CHARACTER COUNT

27674 Characters

PAGE COUNT

6 Pages

FILE SIZE

2.0MB

SUBMISSION DATE

Jul 23, 2023 4:22 PM GMT+7

REPORT DATE

Jul 23, 2023 4:23 PM GMT+7

0% Overall Similarity

This submission did not match any of the content we compared it against.

- 0% Internet database
- 0% Publications database
- Crossref database
- Crossref Posted Content database

Excluded from Similarity Report

- Submitted Works database
- Bibliographic material
- Quoted material
- Cited material
- Small Matches (Less then 40 words)
- Manually excluded text blocks

Materials Science for Energy Technologies 7 (2024) 29–34

Contents lists available at ScienceDirect

Materials Science for Energy Technologies

journal homepage: www.keaipublishing.com/en/journals/materials-science-for-energy-technologies

Design and fabrication of photovoltaics based on MFS (Ag/$BaTiO_3$/silicon p-type) structure

Irzaman [a,*], M. Dahrul [a], M. Rahmani [a], A.M. Rukyati [a], Samsidar [b], Nurhidayah [b], F. Deswardani [b], M. Peslinof [b], R.P. Jenie [c], J. Iskandar [d], Y. Wahyuni [d], K. Priandana [e], R. Siskandar [f,*]

[a] Department of Physics, Faculty of Mathematics and Natural Sciences, IPB University, Bogor 16680, Indonesia
[b] Department of Physics, Faculty of Sciences and Technology, Jambi University, Jambi 36361, Indonesia
[c] Department of Nutrition, Faculty of Health Science and Technology, Binawan University, East Jakarta 13630, Indonesia
[d] Department of Computer Engineering, Pakuan University, Bogor 16142, Indonesia
[e] Department of Computer Science, IPB University, Bogor 16680, Indonesia
[f] Computer Engineering Technology Study Program, College of Vocational Studies, IPB University, Bogor, West Java 16151, Indonesia

ARTICLE INFO

Keywords:
Thin films
$BaTiO_3/Si_{(100)}$
$Li(CH_3COO)$
Photovoltaics

ABSTRACT

The experiment was carried out by growing $BaTiO_3$ (Undoped or Li-doped) on p-type $Si_{(100)}$ substrates using the Chemical Solution Deposition (CSD) method and spin coating at a rotational speed of 3000 rpm for 60 s, followed by heating at 850 °C. The characterization results show that the bandgap energy value of the thin film due to lithium doping reduces the bandgap energy value. This is presumably because the donor atom added to a semiconductor causes the allowable energy level to be slightly below the conduction band. The presence of this new band causes the thin film bandgap energy to decrease with a five-valent tantalum dip. The morphological properties showed that the $BaTiO_3/Si_{(100)}$ thin film particles in the deposited lithium had a fairly homogeneous grain. With the addition of lithium acetate as a binder into barium titanate, the grain size is getting smaller because it is suspected that the lithium-ion radius is smaller than the barium-ion radius. Measurement of I-V on the thin film shows that the output voltage value increases with more light intensity hitting the surface of the thin film. The greater the light intensity, the greater the energy of the photons, so the electrons are easier to jump. The three things above (both electrical and morphological properties) conclude that the thin films grown have the potential for photovoltaics.

1. Introduction

The Ferroelectric materials are materials that undergo spontaneous polarization due to an external electric field [1,2]. The phenomenon of ferroelectricity was first discovered by Valasek in 1912 in Rochelle salt. Ferroelectric is a part of a non-centrosymmetric crystal that has spontaneous polarization. Materials that have ferroelectric properties, in general, are materials in the form of perovskite. Perovskite structure is a simple crystal structure in the form of a cube with the chemical formula $A + 2B + 2O_3^{2}$. Atom A represents a cation with a large ionic radius, B is a cation with a small ionic radius and O is an oxygen atom [3].

Barium titanate ($BaTiO_3$) or often abbreviated as BT is a material that has a perovskite structure. The B atom occupies the A position and the Ti atom occupies the B position in the perovskite crystal structure. When an electric field is applied to the BT, the total charge distribution is not equal to zero, resulting in an excess charge on one side of the crystal which is called polarization. It is characterized by the central atom of the crystal moving to a position corresponding to the direction of the given electric field. BT material is polarized (ferroelectric) when it is below the Curie temperature and is paraelectric when it is above the Curie temperature [4,5].

In addition to having ferroelectric properties, BST thin films have

* Corresponding authors.
E-mail addresses: irzaman@apps.ipb.ac.id (Irzaman), dahrul22@gmail.com (M. Dahrul), meilini_rahmani@gmail.com (M. Rahmani), anis_68@apps.ipb.ac.id (A.M. Rukyati), samsidar@unja.ac.id (Samsidar), nurhidayah@unja.ac.id (Nurhidayah), frastica.deswardani@unja.ac.id (F. Deswardani), mardianpeslonof@unja.ac.id (M. Peslinof), qwerty.user1983@gmail.com (R.P. Jenie), johan_iskandar@unpak.ac.id (J. Iskandar), yuli_wahyuni@unpak.ac.id (Y. Wahyuni), kpriandana@gmail.com (K. Priandana), ridwansiskandar@apps.ipb.ac.id (R. Siskandar).

https://doi.org/10.1016/j.mset.2023.06.002
Received 3 May 2023; Received in revised form 27 June 2023; Accepted 27 June 2023
Available online 7 July 2023

sensitivity to light (optoelectronics), sensitivity to temperature stimuli (pyroelectric), and sensitivity to pressure effects (piezoelectric) [1,6–8]. Pyroelectric properties have been applied as infrared thermal switches and infrared sensors. The properties of BST have been applied as an optoelectronic photodiode [9]. In addition, its sensitivity to light has been applied in automatic drying models in agriculture [1,10].

The dopant is a material that is expected to be able to change the lattice constant, dielectric constant, pyroelectric properties, optoelectronic properties, and piezoelectric properties of ceramics and BST thin films for the better. Dopant classification can be distinguished according to its elements, namely soft dopant and hard dopant. Soft dopant ions make ferroelectric materials have a high coefficient of elasticity, low coercive field properties, and lower mechanical quality factor. Hard dopant ions can produce harder ferroelectric materials such as lower dielectric loss, lower bulk resistivity, higher coercive field properties, higher mechanical quality factor, and higher electrical quality factor [3,11].

BT thin films have been made by several techniques such as sputtering, laser ablation, and sol–gel process [12–15], while CuO thin films can be made by several coating techniques such as dip- coating, vacuum evaporation, a sputtering process, chemical solution deposition (CSD). The CSD method is very interesting to develop because it has good stoichiometric control, is easy to fabricate, and is synthesized at room temperature [11,16–18].

The CSD method is a method of growing a thin layer using a chemical solution on the surface of the substrate at room temperature. This method is cheaper because it does not need a vacuum, has good stoichiometric control, is easy to manufacture, and is very good for research on a laboratory scale. The main advantage of the CSD method is that the material or film that can be made is produced at the final mixture composition at the molecular level so that the diffusion time of the material after undergoing the pyrolysis process to achieve thermodynamic equilibrium is quite short and stable. This resulted in the results obtained were homogeneous mixtures and thick films [18].

The research aimed to synthesize and characterize $BaTiO_3/Si_{(1\,0\,0)}$ thin films in lithium doped with potential as solar cells.

2. Material and methods

2.1. Research settings

The materials used in this research include p-type silicon (Si) substrate (1 0 0), Barium titanate ($BaTiO_3$) powder, Barium oxide (BaO) powder, Lithium acetate powder [$Li(CH_3COO)$, 99%], solvent 2-methoxy ethanol [$C_3H_8O_2$, 99%], Aquabides, Methanol, Acetone, and dish soap. This study uses several equipment, namely insulated boxes, double-sided tape, solution, paper labels, stationery, scissors, solution bottles, diamond blades, tweezers, weighing paper, digital balance, gloves, masks, micropipettes, tissue, aluminum foil, stirrer, spatula, Ultrasonic cleaner Bransonic 5800 (Branson, USA), X-Ray Diffraction (XRD) X'Pert PRO (PANalytical, United Kindom), Nabertherm Furnace Vulcan$^{TM\ 3\text{-}130}$ (Nabertherm, Germany) and Scanning Electron Microscopy (SEM-EDX) Inspect-S50 (FEI, Japan).

2.2. Thin film synthesis

The substrate used in the manufacture of thin films in this study is a p-type (1 0 0) silicon (Si) substrate. The substrate was then cut to a size of 1.2 cm × 1.2 cm using a diamond blade. Next, the substrate was weighed using a digital balance with 3 repetitions for each substrate. After weighing, the substrate was washed using aquabides solution with dish soap, methanol, and acetone. Substrate washing consists of 3 stages with different solutions with the help of an ultrasonic cleaner. The substrate washing time for each solution is about 5–10 min. Before washing with another solution, the Si(1 0 0) substrate must be dried on a hotplate.

Preparation of the solution begins with preparing powdered Barium titanate ($BaTiO_3$), powdered Barium oxide (BaO) as stoichiometric equaliser, powdered Lithium acetate [$Li(CH_3COO)$, 99%], and solvent 2-methoxy ethanol [$C_3H_8O_2$, 99%]. The ingredients are weighed according to the composition of the ingredients (1). Thin film growth using The material that has been weighed is then put into a solution bottle. After that, the stirring process was carried out using a magnetic stirrer for 60 min. The solution was prepared with a variation of 0% and 1.5% in 4 bottles of different solutions according to the composition in Table 1.

$$0.985BaTiO_3 + 0.015Li(CH_3COO) + 0.015BaO + 0.04125O_2 \text{ - -> } BaTi_{0,985}Li_{0,015}O_3 + 0{\cdot}.0225H_2O + 0.03CO_2 \quad (1)$$

Thin film growth using Chemical Solution Deposition (CSD) method with spin coating technique. The silicon substrate is placed on a spin coater plate using double-sided tape. Half of the substrate is then covered with tape, then the part that is not covered with tape is dripped with the previously prepared solution. The spin coater is rotated with a rotating speed setting of 3000 rpm for 60 s.

The annealing step aims to diffuse the thin film solution with a silicon substrate. The heating process begins at room temperature and then is raised to a temperature of 850 °C with an increased rate of 1.67 °C/minute, then held constant at that temperature for 8 h. Then the temperature is returned to room temperature. The process of raising the room temperature to 850 °C takes ± 8.5 h, while it takes 12 h to lower the temperature back to room temperature.

2.3. General characterization

X-ray diffraction measurements in this study used an angle of incidence of 2θ at an interval of 20° to 80° with an interval of 0.02°/minute. The lattice parameter analysis of the XRD spectral experimental data was analyzed using the Cramer and Cohen equations [18–20]. The resulting XRD data is analyzed to determine the crystal size of each material phase [21,22]. The XRD has been analysed using ICDD No 05–0626 as comparison.

The SEM test was carried out to determine the surface morphology of the thin films that had been made using a magnification of 40,000 times. At the time of this research, we did not have access to better precision SEM device, which could enable 100,000 magnification. Further observation is needed. The EDX test was carried out to find out what elements were contained in the thin film that had been synthesized in this study [23–25]. AFM testing was carried out to determine the microstructure of the thin layer. From the AFM test, the RMS value will be obtained which indicates the smoothness of the film surface [26,27].

Energy gap analysis was carried out using the Kubelka Munk. The Kubelka Munk is one of the methods used in analyzing the energy gap of a semiconductor material. The energy band gap values are determined with the Kubelka Munk method with line drawing straight between absorption coefficient (hυ) and absorption coefficient to photons ($\alpha_{K\text{-}M}h\upsilon^2$) [28-31].

Space Charge Limited Current (SCLC) analysis was used to measure the optoelectronic and charge carrier transport properties of perovskite crystals. The addition of doped on the thin film will increase the electron mobility [32].

The Nyquist plot was conducted to determine the strength of the electrical properties of semiconductor thin films [33].

Photovoltaics Potential Analysis of Diode which Made of Thin Film BaTiO3/Si(1 0 0) with Lithium test was carried out to determine the sensitivity of the thin film to the response of light intensity (strong).

Table 1
Composition of materials for making $BaTiO_3$ solution at a solubility of 1 M.

Variation Container	$BaTiO_3/Si_{(1\,0\,0)}$ (g)	BaO (g)	$Li(CH_3COO)$ (g)	2-metoxy-etanol (ml)
0%	0.4664	0	0	2
1.5%	0.4594	0.0046	0.0020	2

Testing will be carried out at an intensity of 1000 lx and 2000 lx. So that finally it can be concluded whether this thin film can be potential and implemented as photovoltaic.

3. Result and discussions

The XRD pattern of the test results describes the splitting of the diffraction peaks at 31° according to a plane (1 1 0) (Fig. 1). The results show that the thin films (without doping and with 1.5% doping) have a tetragonal structure.

Based on Fig. 1 and the Cramer and Cohen equations, the $BaTiO_3$ without lithium has a tetragonal structure with lattice parameters a = b = 3.987 Å; c = 4.099 Å, while $BaTiO_3$ with lithium has a tetragonal structure with lattice parameters a = b = 3.958 Å; c = 3.996 Å. this result is close to ICDD No 05-0626.

The $BaTiO_3$/Si(1 0 0) thin film particles in the deposited lithium have granulated grain (Fig. 2), which is quite homogeneous. The calculated particle diameter of the $BaTiO_3$/Si(1 0 0) thin film without Lithium is about 0.2 nm, while with 1.5% Lithium is about 0.16 nm, based on the particle size distribution in each Figure. With the addition of a percentage of lithium acetate dopant as a binder into barium titanate, the grain size is getting smaller. It is suspected that the lithium-ion radius (0.8 Å) is smaller than the barium ion radius (2.22 Å).

The EDX results do not get lithium atoms because the lithium atoms have a small atomic number so the energy emitted by lithium is not captured by the EDX (Fig. 2). The composition of the material contained in the $BaTiO_3$/Si(1 0 0) thin film in Lithium is 43.03% Ba, 2.01% Si, 8.76 % N, and 46% O. The composition of the material contained in the $BaTiO_3$/Si(1 0 0) thin film with Lithium is 39.71% Ba, 0.94% Si, 6.23 % N, and 53% O. The results of this EDX analysis show that the $BaTiO_3$/Si (1 0 0) film is not stoichiometric, because the lithium atom has a small atomic number so the energy emitted by lithium is not captured by the EDX.

AFM testing on $BaTiO_3$/Si(1 0 0) thin films doped with 0% and 1.5% lithium to determine the microstructure of the thin films. The statistical analysis of the surface roughness without doping and with 1.5% doping respectively 150 nm, and 109 nm (Fig. 2). Root Mean Squared (RMS) decreased with additional lithium doping. This shows that the surface of the thin film with 1.5% doping is smoother. The RMS value has shown that the surface is quite rough.

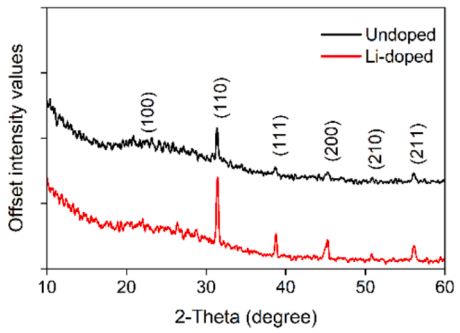

a. XRD Pattern of BaTiO3/Si(100) thin film Crystal Structure.

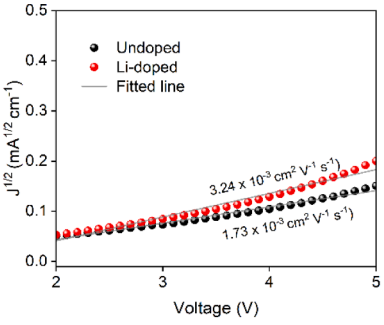

b. $BaTiO_3/Si_{(100)}$ with 1.5% Li(CH_3COO) dopant Electron mobility using the SCLC method..

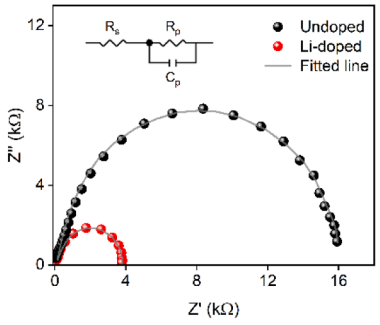

c. $BaTiO_3/Si_{(100)}$ with no dopant Nyquist plot

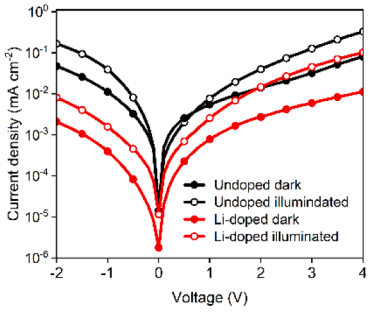

d. $BaTiO_3/Si_{(100)}$ with 1.5% Li(CH_3COO) dopant Photovoltaics Potential

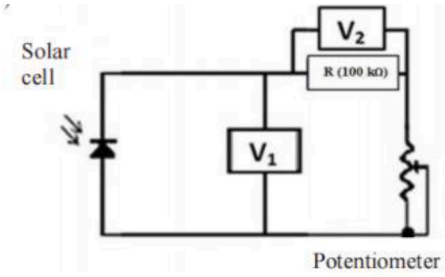

e. Ag/$BaTiO_3$/Si(100) thin film-based solar cell structure in Lithium

Fig. 1. XRD and electrical characteristics of $BaTiO_3/Si_{(1\,0\,0)}$ thin film crystal.

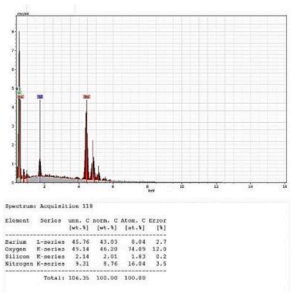

a. $BaTiO_3$/Si(100) with no dopant material composition.

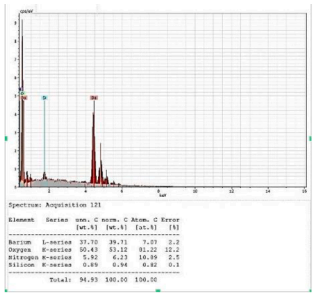

b. $BaTiO_3$/Si(100) with 1.5% $Li(CH_3COO)$ dopant Material Composition.

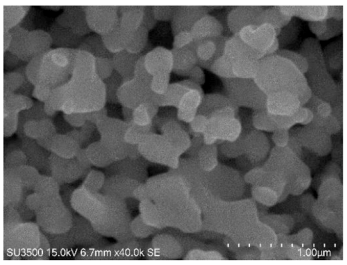

c. $BaTiO_3$/Si(100) with no dopant morphology

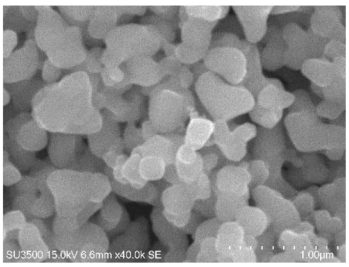

d. $BaTiO_3$/Si(100) with 1.5% $Li(CH_3COO)$ dopant morphology

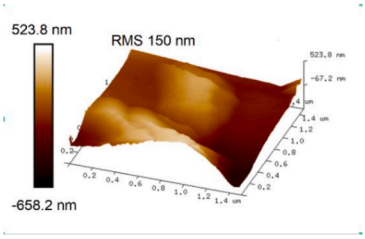

e. $BaTiO_3$/Si(100) with no dopant AFM

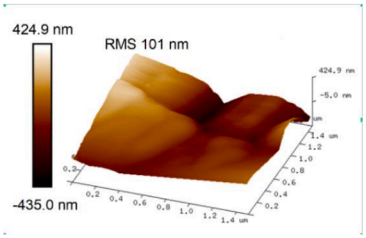

f. $BaTiO_3$/Si(100) with 1.5% $Li(CH_3COO)$ dopant AFM

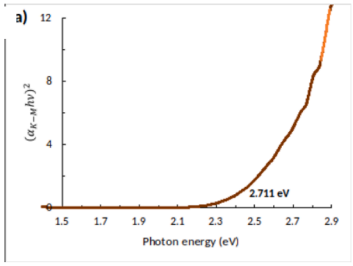

g. $BaTiO_3$/Si(100) with no dopant energy gap

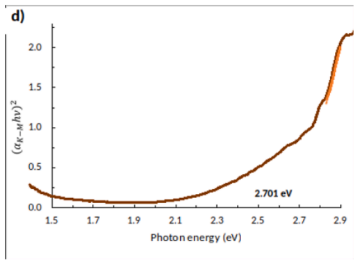

h. $BaTiO_3$/Si(100) with 1.5% $Li(CH_3COO)$ dopant energy gap

Fig. 2. General characteristics of $BaTiO_3/Si_{(1\,0\,0)}$ thin film crystal.

The addition of $Li(CH_3COO)_2$) leads to an increase in the electrical conductivity of the film, thereby decreasing the energy gap value (Fig. 2). When a donor atom is added to a semiconductor, the permissible energy level will be slightly below the conduction band. The presence of this new band causes the thin film bandgap energy to decrease with five-valent lithium doped [17]. The lithium doping applied to the $BaTiO_3$ thin film reduces the energy gap of the thin film because the electrons generated in the conduction band decrease. Based on previous research, it has been stated that the energy gap can increase after adding a lithium filler [34].

Increasing the amount of Li doping indicates a significant increase in electron mobility (Fig. 1). Electron mobility on Li 1.5% showed higher mobility (3.24×10^{-3} cm2 V^{-1} s^{-1}) when compared to electron mobility without doping Li (1.73×10^{-3} cm2 V^{-1} s^{-1}). This is consistent with the increase in crystallinity shown in Fig. 1. The XRD graph shows a sharp peak at (1 1 0), associated with the highest degree of crystallinity among thin films analyzed in this study. In conclusion, in relatively low doping (Li 1.5%), carrier concentration increases linearly with doping concentration, resulting in increased conductivity.

Nyquist plots for Li 0% and Li 1.5% devices were carried out over the frequency range from 100 Hz to 1 MHz (Fig. 1), where the imaginary impedance (Z'') is plotted against the real impedance (Z'). The minimum Z value in the Nyquist plot indicates the contact resistance at the electrodes, i.e. is shown as the series resistance (Rs) whereas Rp indicates the equivalent charge resistance (Fig. 1). the amount of Li doping increased by 1.5% resulting in a 3/4 circle size in our set Nyquist plot shrinking (Table 2).

Measurement of the I-V curve was carried out to find out whether $BaTiO_3$ can be used as a photosensitive coating. The measurement results are determined by two index values, namely photocurrent density

Table 2
EIS parameters of Li(CH_3COO)-doped $BaTiO_3$ devices were obtained by fitting the Nyquist plots with the equivalent circuit.

Sample	Rs	Rp	Cp (nF)
0% (undoped)	151.6 ± 15.306	15640 ± 3.226	0.651 ± 3.839
1.5% (Li doped)	100.3 ± 9.4951	3750 ± 0.861	0.697 ± 1.953

and dark current density (Jlight/Jdark). To observe the trend of illumination of light and dark currents at various voltages. $BaTiO_3$ without Li doping (0%) was chosen as the reference set, and $BaTiO_3$ with 1.5% Li doping concentration was used as the comparison set (Fig. 1). This confirms that Li-doped $BaTiO_3$ thin films can be used as photodetectors or photovoltaics.

Tests of electrical and morphological properties of $BaTiO_3$/Si(1 0 0) thin films with 0% and 1.5% lithium doping showed that thin films with 1.5% lithium doping were the best films, which were then assumed to have the potential to be implemented as solar cells. The manufacture of solar cells made of $BaTiO_3$/Si(1 0 0) thin film in lithium 1.5% is done by adding aluminum contacts on a substrate of silicon Si(1 0 0) and barium titanate so that the structure of Ag/$BaTiO_3$/Si(1 0 0) is formed. The arrangement of solar cells formed resembles a sandwich, as shown in Fig. 1. Then the current and voltage characterization of the solar cell samples that have been formed is carried out. To measure current and voltage, an ammeter and voltmeter are used.I-V measurements were carried out in two conditions, namely when there was no light and when the solar cell was exposed to light. When a solar cell is exposed to light, there will be a generation (the emergence of electron-hole pairs). The photons absorbed by the electrons on the surface cause the electrons to be excited and then the electrons flow towards the holes through the metal contact layer.

This metallic contact layer becomes a pathway for electrons to flow faster toward the holes. Furthermore, electrons flow through the external load to the counter electrode and will be accepted by the electrolyte. While the holes formed will diffuse into the electrolyte. This means that electrons received by the electrolyte will recombine with holes to form negative charge carriers. In this study, the only thing that can be measured is the voltage of the solar cell. While the current can not be measured because the order is still very small. Therefore, it is not possible to display the I-V curve of each solar cell sample made so the efficiency is not yet known. Lithium added to the film layer produces an increasing stress value (Table 3). I-V measurements were carried out in dark conditions (0 lx), and bright conditions with light intensities of 1000 lx and 2000 lx. The output voltage values of each thin film with different lithium doping concentrations (0% and 1.5%). The voltage output increases with more light intensity hitting the thin film surface. The greater the light intensity, the greater the energy of the photons, so the electrons are easier to jump. This is in line with what has been done by previous researchers, and has succeeded in implementing thin films as light-sensitive sensors [1,7,9,10,35].

The data on the characterization of the $BaTiO_3$/Si(1 0 0) thin film in lithium include (i) the results of XRD pattern analysis; (ii) Gap energy from optical properties test; (iii) SEM/EDAX analyzers; (iv) I-V measurement results of thin-film solar cells from electrical properties test show that $BaTiO_3$/Si(1 0 0) thin films in lithium-ion have potential as solar cells.

4. Conclusions

The morphology, crystal structure, and electrical and optoelectronic properties of the devices were studied systematically. Li-doped BTO thin films exhibit a pure tetragonal perovskite structure. With the introduction of Li doping, a smoother thin film is achieved and the electron mobility of BTO is increased. The bandgap energy value of the thin film due to lithium doping reduces the bandgap energy value. This is presumably because the donor atom added to a semiconductor causes the allowable energy level to be slightly below the conduction band. The presence of this new band causes the thin film bandgap energy to decrease with a five-valent tantalum dip. The morphological properties showed that the $BaTiO_3$/Si(1 0 0) thin film particles in the deposited lithium had a fairly homogeneous grain. With the addition of lithium acetate as a binder into barium titanate, the grain size is getting smaller because it is suspected that the lithium-ion radius is smaller than the barium-ion radius. Measurement of I-V on the thin film shows that the output voltage value increases with more light intensity hitting the surface of the thin film. The greater the light intensity, the greater the energy of the photons, so the electrons are easier to jump. The four things above (both electrical and morphological properties) conclude that the thin films grown have the potential for photodetectors and photovoltaics.

Table 3
I-V measurement results of thin-film solar cells.

Lithium Container (%)	Rated voltage (volt)		
	0 lx	1000 lx	2000 lx
0	0.000	0.0145	0.0162
1.5	0.000	0.1732	0.1975

CRediT authorship contribution statement

Irzaman: Conceptualization, Project administration. **M. Dahrul:** Supervision, Resources. **M. Rahmani:** Writing – review & editing. **A.M. Rukyati:** Writing – original draft, Project administration. **Samsidar:** Methodology. **Nurhidayah:** Formal analysis. **F. Deswardani:** Validation. **M. Peslinof:** Writing – review & editing. **R.P. Jenie:** Writing – review & editing. **J. Iskandar:** Writing – original draft, Project administration. **Y. Wahyuni:** Writing – original draft, Project administration. **K. Priandana:** Validation. **R. Siskandar:** Writing – original draft.

Declaration of Competing Interest

The authors declare that they have no known competing financial interests or personal relationships that could have appeared to influence the work reported in this paper.

Acknowledgements

This research was funded by the IPB Rectorate Research Grant for the Collaborative Research Program Universitas Jambi dan Institut Pertanian Bogor with contract number: 4010/IT3.L1/PT.01.03/M/T/2022 on 7 June 2022.

References

[1] R.S. Irzaman, I. Aminullah, H. Alatas, Characterization of Ba0.55Sr0.45TiO3 films as light and temperature sensors and its implementation on automatic drying system model, Integr. Ferroelectr. 168 (2016) 130–150, https://doi.org/10.1080/10584587.2016.1159537.
[2] M. Pratheek, T. Abhinav, S. Bhattacharya, G.K. Chandra, P. Predeep, Recent progress on defect passivation in perovskites for solar cell application, Mater. Sci. Energy Technol. 4 (2021) 282–289, https://doi.org/10.1016/j.mset.2021.07.003.
[3] M. Falmbigl, I.S. Golovina, A.V. Plokhikh, D. Imbrenda, A. Podpirka, C.J. Hawley, G. Xiao, A. Gutierrez-Perez, I.A. Karateev, A.L. Vasiliev, T.C. Parker, J.E. Spanier, BaTiO3 thin films from atomic layer deposition: a superlattice approach, J. Phys. Chem. C. 121 (2017) 16911–16920, https://doi.org/10.1021/acs.jpcc.7b05633.
[4] A. Karvounis, F. Timpu, V.V. Vogler-Neuling, R. Savo, R. Grange, Barium titanate nanostructures and thin films for photonics, Adv. Opt. Mater. 8 (2020) 1–23, https://doi.org/10.1002/adom.202001249.
[5] Q. Wang, L.Y. Niu, J.Y. Jing, W.M. Zhao, Barium titanate film based fiber optic surface plasmon sensor with high sensitivity, Opt. Laser Technol. 124 (2020), 105899, https://doi.org/10.1016/j.optlastec.2019.105899.
[6] Irzaman, Ridwan Siskandar, Brian Yuliarto, Mochammad Zakki Fahmi, Ferdiansjah, Application of Ba 0 . 5 Sr 0 . 5 TiO 3 (Bst) Film Doped with Arduino Nano-Based Bad Breath Sensor, Chemosensor. 3 (2020) 1–11.
[7] R. Siskandar, F.C. Dio, H. Alatas, Irzaman, Application of Ba0.5Sr0.5TiO3 (BST) film doped with RuO2 (0%, 2%, 4% and 6%) on a rice-stalk cutting robot model

based on a line follower with Hc-05 bluetooth control, Biointerface Res. Appl. Chem. 12 (2022) 2138–2151.
[8] V.X.T. Zhao, T.I. Wong, X.T. Zheng, Y.N. Tan, X. Zhou, Colorimetric biosensors for point-of-care virus detections, Mater. Sci. Energy Technol. 3 (2020) 237–249, https://doi.org/10.1016/j.mset.2019.10.002.
[9] Irzaman, R. Siskandar, R.P. Jenie, H. Syafutra, M. Iqbal, B. Yuliarto, M.Z. Fahmi, Ferdiansjah, Khairurrijal, Ferroelectric sensor BaxSr1-xTiO3 integrated with android smartphone for controlling and monitoring smart street lighting, J. King Saud Univ. - Sci. 34 (2022) 102180. doi: 10.1016/j.jksus.2022.102180.
[10] R. Siskandar, T. Mandang, W. Hermawan, I. Irzaman, Thin film potential Ba0.5Sr0.5 TiO3 (BST) doped with RuO2 6% as a light detecting sensor at solar tracker ALSINTAN system in microcontroller-based, Biointerface Res. Appl. Chem. 13 (2023) 1–15, https://doi.org/10.33263/BRIAC136.545.
[11] S.W. Konsago, K. Žiberna, B. Kmet, A. Benčan, H. Uršič, B. Malič, Chemical solution deposition of barium titanate thin films with ethylene glycol as solvent for barium acetate, Molecules 27 (2022) 3753, https://doi.org/10.3390/molecules27123753.
[12] S.I. Gudkov, A.V. Solnyshkin, D.A. Kiselev, A.N. Belov, Electrical conductivity of lithium tantalate thin film, Ceramica 66 (2020) 291–296, https://doi.org/10.1590/0366-69132020663792885.
[13] A.M. Moreira Ficanha, A. Antunes, C.E. Demaman Oro, R.M. Dallago, M. L. Mignoni, Immobilization of Candida antarctica B (CALB) in silica aerogel: morphological characteristics and stability, Biointerface Res. Appl. Chem. 10 (2020) 6744–6756, https://doi.org/10.33263/BRIAC106.67446756.
[14] B.K. Swamy, K. Shiprath, K.V. Ratnam, H. Manjunatha, S. Janardan, A. Ratnamala, K.C.B. Naidu, S. Ramesh, K.S. Babu, Electrochemical detection of dopamine and tyrosine using metal oxide (MO, M=Cu and Ni) modified graphite electrode: a comparative study, Biointerface Res. Appl. Chem. 10 (2020) 6460–6473, https://doi.org/10.33263/BRIAC105.64606473.
[15] A. Ranjitha, M. Thambidurai, F. Shini, N. Muthukumarasamy, D. Velauthapillai, Effect of doped TiO2 film as electron transport layer for inverted organic solar cell, Mater. Sci. Energy Technol. 2 (2019) 385–388, https://doi.org/10.1016/j.mset.2019.02.006.
[16] P.L. Bintari, V. Rahmawaty, E.K. Palupi, N. Patonah, T.S. Irmansyah, Irzaman, Effect of light intensity on magnetic properties of srtio3 thin-films, Key Eng. Mater. 855 KEM (2020) 208–212, https://doi.org/10.4028/www.scientific.net/KEM.855.208.
[17] X. Tang, K.H. Li, C.H. Liao, J.M. Taboada Vasquez, C. Wang, N. Xiao, X. Li, Chemical solution deposition of epitaxial indium- and aluminum-doped Ga2O3 thin films on sapphire with tunable bandgaps, J. Eur. Ceram. Soc. 42 (2022) 175–180, https://doi.org/10.1016/j.jeurceramsoc.2021.09.064.
[18] Y. Iriani, F. Nurosyid, A.U.L.S. Setyadi, The effect of mole concentrations of Sr-doped of BAI. X Sr x TiO3 film on microstructure, optical, and electrical properties, AIP Conf. Proc. 2296 (2020), https://doi.org/10.1063/5.0032543.
[19] A. Setiawan, E.K. Palupi, R. Umam, H. Alatas, Irzaman, Optical characterization of Ba0.5Sr0.5TiO3 material grown on a p-type silicon substrate (111) doped niobium oxide and chlorophyll, Ferroelectrics 568 (2020) 62–70, https://doi.org/10.1080/00150193.2020.1735893.
[20] H.A. Elazab, M.N. Ayad, M.M. Hammam, M.A. Radwan, M.A. Sadek, Synthesis and characterization of PVP based catalysts for selected application in catalysis, Biointerface Res. Appl. Chem. 10 (2020) 5209–5216, https://doi.org/10.33263/BRIAC102.209216.
[21] E.K. Droepenu, B.S. Wee, S.F. Chin, K.Y. Kok, E.A. Asare, Synthesis and characterization of single phase ZnO nanostructures via solvothermal method: influence of alkaline source, Biointerface Res. Appl. Chem. 10 (2020) 5648–5655, https://doi.org/10.33263/BRIAC103.648655.
[22] A. Tripathy, M. Behera, A.S. Rout, S.K. Biswal, A.D. Phule, Optical, structural, and antimicrobial study of gold nanoparticles synthesized using an aqueous extract of Mimusops elengi raw fruits, Biointerface Res. Appl. Chem. 10 (2020) 7085–7096, https://doi.org/10.33263/BRIAC106.70857096.
[23] A. Massit, A. El Yacoubi, A. Rezzouk, B.C. El Idrissi, Thermal behavior of Mg-doped calcium-deficient apatite and stabilization of beta tricalcium phosphate, Biointerface Res. Appl. Chem. 10 (2020) 6837–6845, https://doi.org/10.33263/BRIAC106.68376845.
[24] A. Hamdani, M. Komaro, Irzaman, A synthesis of BaXSr1-xTiO3 film and characterization of ferroelectric properties and its extension as random access memory, Mater. Phys. Mech. 42 (2019) 131–140, https://doi.org/10.18720/MPM.4212019_11.
[25] M.H. Rajvee, S.V. Jagadeesh Chandra, P. Rajesh Kumar, C.H.V.V. Ramana, K. Neelama, R.S. Dubey, Synthesis and analysis of zirconium titanate thin films by using sol-gel method, Biointerface Res. Appl. Chem. 11 (2021) 12761–12768, https://doi.org/10.33263/BRIAC115.1276112768.
[26] S.N.A. Bakil, H. Kamal, H.Z. Abdullah, M.I. Idris, Sodium alginate-zinc oxide nanocomposite film for antibacterial wound healing applications, Biointerface Res. Appl. Chem. 10 (2020) 6289–6296, https://doi.org/10.33263/BRAIC105.62456252.
[27] Y.R. Liu, L.F. Ren, R.H. Yang, J. Han, R.H. Yao, Z.C. Wen, H.H. Xu, J.X. Xu, Effects of annealing temperature on electrical properties of ZnO thin-film transistors, Nanomaterials. 12 (2022) 1–11, https://doi.org/10.3969/j.issn.1000-565X.2011.09.018.
[28] D.Q.G. Ds, D. Rq, Q. Gmrkdq, X. Df, The Optical Band Gap Based on K-M Function on Layer of LiTaO3 with Variation Treatment of Annealing Temperature, 7 (n.d.) 7–10.
[29] V.N. Vikash Mishra, Aanchal Sati, M. Kamal Warshi, Ambadas B. Phatangare, Sanjay Dhole, R.K. and P.R. Bhoraskar, Harnath Ghosh, Archna Sagdeo, Vinayak Mishra, 9, Sagdeo, Effect of electron irradiation on the optical properties of SrTiO3: An experimental and theoretical investigations, (2018).
[30] A. Kurniawan, Irzaman, B. Yuliarto, M.Z. Fahmi, Ferdiansjah, Application of barium strontium titanate (BST) as a light sensor on led lights, Ferroelectrics 554 (2020) 160–171, https://doi.org/10.1080/00150193.2019.1684758.
[31] A.M. Abdelghany, D.M. Ayaad, S.M. Mahmoud, Antibacterial and energy gap correlation of PVA/SA biofilms doped with selenium nanoparticles, Biointerface Res. Appl. Chem. 10 (2020) 6280–6288, https://doi.org/10.33263/BRIAC105.62366244.
[32] A. Thakre, A. Kumar, Enhanced bipolar resistive switching behavior in polar Cr-doped barium titanate thin films without electro-forming process, AIP Adv. 7 (2017), https://doi.org/10.1063/1.5004232.
[33] K. Auromun, R.N.P. Choudhary, Structural, dielectric and electrical investigation of zirconium and tin modified 0.5BFO-0.5BST, Mater. Chem. Phys. 250 (2020), 123033, https://doi.org/10.1016/j.matchemphys.2020.123033.
[34] A. Ismangil, W.G. Prakoso, The Effect of Electrical Conductivity of LiTaO 3 Thin film to Temperature Variations, 29 (2020) 3234–3240.
[35] R. Irzaman, N.N. Siskandar, B. Aminullah, K.A. Yuliarto, H.A. Hamam, Application of lithium tantalate (LiTaO3) films as light sensor to monitor the light status in the Arduino Uno based energy-saving automatic light prototype and passive infrared sensor, Ferroelectrics 524 (2018) 44–55, https://doi.org/10.1080/00150193.2018.1432842.

0% Overall Similarity

NO MATCHES FOUND

This submission did not match any of the content we compared it against.

Excluded from Similarity Report

- Submitted Works database
- Quoted material
- Small Matches (Less then 40 words)
- Bibliographic material
- Cited material
- Manually excluded text blocks

EXCLUDED TEXT BLOCKS

Chemical Solution Deposition (CSD) method and spin coating at a rotational speed...

Irzaman, M. Dahrul, M. Rahmani, A.M. Rukyati et al. "Design and Fabrication of Photovoltaics Based on MFS ...

photovoltaics.1. IntroductionThe Ferroelectric materials are materials that underg...

Irzaman, M. Dahrul, M. Rahmani, A.M. Rukyati et al. "Design and Fabrication of Photovoltaics Based on MFS ...

sensitivity to light (optoelectronics), sensitivity to temperature stimuli(pyroelectric...

Irzaman, M. Dahrul, M. Rahmani, A.M. Rukyati et al. "Design and Fabrication of Photovoltaics Based on MFS ...

Barium titanate (BaTiO3) powder, Barium oxide (BaO)powder, Lithium acetate pow...

Irzaman, M. Dahrul, M. Rahmani, A.M. Rukyati et al. "Design and Fabrication of Photovoltaics Based on MFS ...

1.2 cm using a diamond blade. Next, the substrate was weighedusing a digital bala...

Irzaman, M. Dahrul, M. Rahmani, A.M. Rukyati et al. "Design and Fabrication of Photovoltaics Based on MFS ...

0.03CO2(1)Thin film growth using Chemical Solution Deposition (CSD) methodwit...

Irzaman, M. Dahrul, M. Rahmani, A.M. Rukyati et al. "Design and Fabrication of Photovoltaics Based on MFS ...

Testing will be carried out at an intensity of 1000

Irzaman, M. Dahrul, M. Rahmani, A.M. Rukyati et al. "Design and Fabrication of Photovoltaics Based on MFS ...

The addition of Li

Irzaman, M. Dahrul, M. Rahmani, A.M. Rukyati et al. "Design and Fabrication of Photovoltaics Based on MFS ...

10-3 cm2 V− 1

Irzaman, M. Dahrul, M. Rahmani, A.M. Rukyati et al. "Design and Fabrication of Photovoltaics Based on MFS ...

Table 2EIS parameters of Li

Irzaman, M. Dahrul, M. Rahmani, A.M. Rukyati et al. "Design and Fabrication of Photovoltaics Based on MFS ...

and dark current density (Jlight/Jdark). To observe the trend of

Irzaman, M. Dahrul, M. Rahmani, A.M. Rukyati et al. "Design and Fabrication of Photovoltaics Based on MFS ...

allowable energy level to be slightly below the conduction band. Thepresence of th...

Irzaman, M. Dahrul, M. Rahmani, A.M. Rukyati et al. "Design and Fabrication of Photovoltaics Based on MFS ...

Declaration of Competing InterestThe authors declare that they have no known co...

Irzaman, M. Dahrul, M. Rahmani, A.M. Rukyati et al. "Design and Fabrication of Photovoltaics Based on MFS ...

Received

os.unil.cloud.switch.ch